

## Limits of Confinement:

# The First 15 Years of Ultra-Relativistic Heavy Ion Studies

H. Satz <sup>a\*</sup>

<sup>a</sup>Fakultät für Physik, Universität Bielefeld,  
Postfach 100 131, D-33501 Bielefeld, Germany

The study of high energy nuclear collisions has entered a new stage with RHIC; it therefore seems a good time to ask what we have learned from the experimental results obtained up to now. I recall what we had expected to find when the SPS and AGS programs were started, summarize what actually was found, and then try to assess what we have learned from the results.

### 1. The Beginning

It all began with the idea of an intrinsic limit to hadron thermodynamics. During the past fifty years, different conceptual approaches had led to an ultimate temperature of strongly interacting matter. Pomeranchuk [ 1] first obtained it from the finite spatial extension of hadrons: a hadron can only have an independent existence if it has an independent volume. Then Hagedorn [ 2] arrived at a limiting temperature by postulating a self-similar hadronic resonance composition: a resonance consists of resonances which consist of resonances, and so on. The resulting excitation spectrum was later also derived in the dual resonance model [ 3]. With the advent of the quark infrastructure of hadrons and of quantum chromodynamics, it became clear that the ultimate temperature found in all these considerations was really a transition point to a new state of matter, to a plasma of deconfined quarks and gluons [ 4].

Statistical QCD, in particular in the finite temperature lattice formulation, has subsequently confirmed this hypothesis: at a now rather well determined temperature (for vanishing baryon density,  $T_c \simeq 150 - 180$  MeV), strongly interacting matter undergoes a transition from a medium of color singlet hadronic constituents to one of deconfined colored quarks and gluons [ 5]. The energy density at the transition point was found to be  $\epsilon(T_c) \simeq 0.7 - 1.0$  GeV/fm<sup>3</sup>. Moreover, the transition turns a hadronic state of spontaneously broken chiral symmetry into a quark-gluon plasma in which this symmetry is restored: at  $T_c$ , the effective constituent quark mass of some 0.3 GeV vanishes, and we recover the bare quark mass of the QCD Lagrangian.

The obvious desire to test this fascinating phase structure of strongly interacting matter first led to the fixed target experiments at the AGS in Brookhaven (with  $\sqrt{s} \simeq 5$  GeV) and at the CERN-SPS (with  $\sqrt{s} \simeq 20$  GeV). In 1986/87, light ion beams on heavy ion targets started the program, and in 1994/95, heavy ion beams followed. Today, much of this program is concluded. So, what have we learned during the past fifteen years? In

---

\*Opening talk at Quark Matter 2002, Nantes, France, July 17 - 24, 2002

this opening talk, I will address that question by asking:

- What did we expect to find?
- What did we find?
- What does that tell us?

In my report, I will first recall briefly the expectations concerning signatures at the beginning of the experimental heavy ion program at the AGS and SPS in 1986 and then summarize what had really been found when it was (in first generation experiments) completed in 2000. Following this, I will try to indicate what conclusions can be drawn from these results, for the conditions reached, from the hard probes of the early stages and from the observed hadronisation pattern at freeze-out.

## 2. Hopes

The evolution of a high energy nucleus-nucleus collision was pictured in the form shown in Fig. 1. After a rather short equilibration time  $\tau_0 \simeq 1$  fm, the presence of a thermalized medium was assumed, and for sufficiently high initial energy densities, this medium would be in the quark-gluon plasma phase.

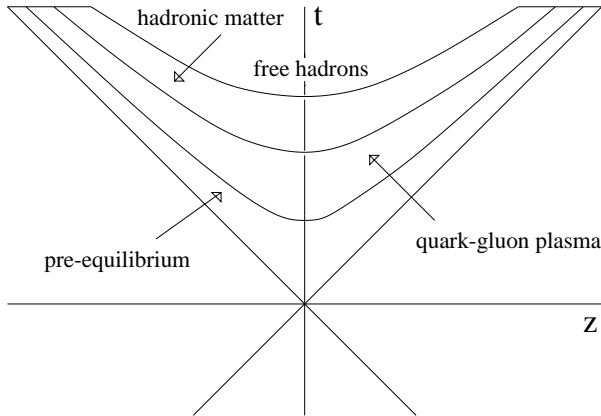


Figure 1. The expected evolution of a nuclear collision

The initial energy density of the produced medium at the time of thermalization was (and still is) generally determined by the Bjorken estimate [ 6]

$$\epsilon = \left( \frac{dN_h}{dy} \right)_{y=0} \frac{w_h}{\pi R_A^2 \tau_0}, \quad (1)$$

where  $(dN_h/dy)_{y=0}$  specifies the number of hadronic secondaries emitted per unit rapidity at mid-rapidity and  $w_h$  their average energy. The effective initial volume is determined in the transverse plane by the nuclear radius  $R_A$ , and longitudinally by the formation time  $\tau_0$  of the thermal medium.

The temperature of the produced medium was assumed to be observable through the transverse mass spectrum of thermal dileptons and the momentum spectrum of thermal photons [ 7, 8]. The observation of thermal dilepton/photon spectra would also indicate

that the medium was indeed in thermal equilibrium. The functional form of the spectra is the same for radiation from hadronic matter and from a QGP; but the observed rates and temperatures were expected to differ in the two cases. It was clear from the beginning that these signals would be emitted during the entire thermal evolution of the system, making a separation of different phases of origin not very straight-forward.

The determination of the nature of the hot initial phase required a signature sensitive to deconfinement. It was argued that in a deconfined medium the  $J/\psi$  would melt through color screening [ 9] and that, therefore, QGP production should lead to a suppression of  $J/\psi$  production in nuclear collisions, compared to the rates extrapolated from  $pp$  data. Similarly, the QGP was expected to result in a higher energy loss for a fast passing color charge than a hadronic medium, so that jet quenching [ 10] should also signal deconfinement.

The behavior of sufficiently short-lived resonances, in particular the dilepton decay of the  $\rho$ , was considered as a viable tool to study the hadronic medium in its interacting stage and thus provide information on the approach to chiral symmetry restoration [ 11].

The expansion of the hot medium was thought to be measurable through broadening and azimuthal anisotropies of hadronic transverse momentum spectra [ 12]. The size and age of the source at freeze-out was assumed to be obtainable through Hanbury-Brown-Twiss (HBT) interferometry based on two-particle correlations [ 13]. It was expected that increasing the collision energy would increase the density and hence the expansion of the produced medium, so that the HBT radii should grow with  $\sqrt{s}$ .

The final interacting hadronic medium was discussed in terms of an ideal resonance gas, following an old suggestion [ 14] brought to hadron physics by Hagedorn [ 2]: an interacting system of elementary constituents can be replaced by a non-interacting gas of resonances, provided the elementary interactions are resonance-dominated. This would provide the relative abundances of all hadron species in terms of just two parameters, the temperature and the baryon number density. One particularly interesting feature here was the fact that in elementary hadronic interactions, an overall reduction of strangeness production was observed. Nuclear collisions, in particular if leading to a QGP as initial stage [ 15], were expected to remove this reduction and lead to strangeness production in accord with thermal predictions.

### 3. Facts

The initial energy density, as specified by the Bjorken estimate, Eq. (1), was measured in almost all SPS experiments. In Fig. 2 we show  $\epsilon$  as function of centrality, determined by the number of participant nucleons [ 16, 17]; it covers the range from somewhat above 1 to almost  $3.5 \text{ GeV/fm}^3$ . Finite temperature lattice calculations, as already mentioned, give for the energy density at deconfinement,  $\epsilon(T_c)$ , values around or slightly below  $1 \text{ GeV/fm}^3$  [ 5]. However, also high energy  $p\bar{p}$  collisions lead to energy density estimates well above  $1 \text{ GeV/fm}^3$ .

Thermal photon or dilepton spectra have so far not been unambiguously identified. Some photon excess over the expected hadronic decay yield has been reported [ 18], but its interpretation is still open. An observed excess of dileptons in the mass range between the  $\phi$  and the  $J/\psi$  [ 19] has been attributed to thermal emission during the evolution of

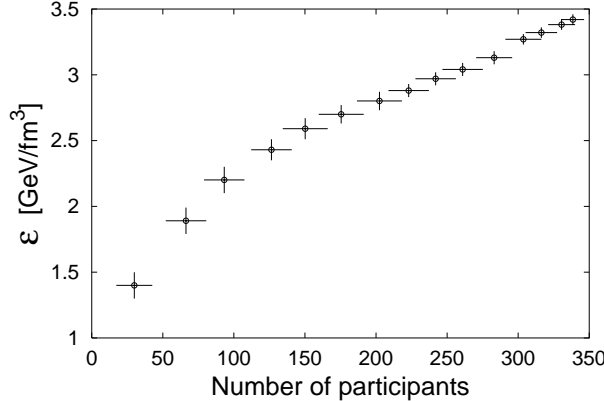


Figure 2. The energy density in Pb-Pb collisions at  $\sqrt{s} = 17$  GeV [ 16, 17].

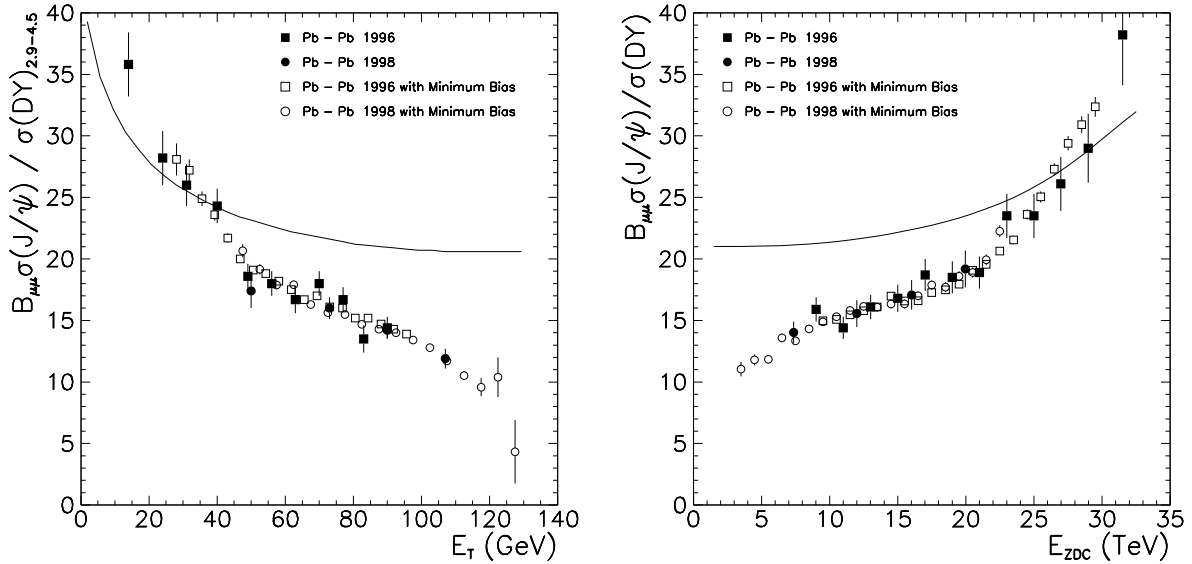


Figure 3. The ratio of  $J/\psi$  to Drell-Yan production, measured by NA50, in Pb-Pb collisions at  $\sqrt{s} = 17$  GeV, vs.  $E_T$  (left) and  $E_{ZDC}$  (right). The solid line indicates the extrapolation of the normal nuclear absorption inferred from p-A collisions [ 16].

the system [ 20], but only a small fraction would be due to the hot early stage; also here, more data is needed to understand the origin of the observed effects.

$J/\psi$  production was found to be suppressed in O-U, S-U and then Pb-Pb collisions; the suppression always increases with centrality [ 21]. Studying p-A collisions, it was observed that already normal nuclear matter leads to reduced charmonium production. Extrapolating this ‘normal’ suppression to  $AB$  interactions is enough to account for the observed yields up to central S-U collisions. In central Pb-Pb collisions, however, an additional ‘anomalous’ suppression was observed [ 16]. Peripheral Pb-Pb collisions follow the normal pattern; then, with increasing centrality (measured either through the associated transverse energy or through the number of participating nucleons), there is a pronounced onset of further suppression (Fig. 3). The very peripheral data points shown in this figure are somewhat above the normal suppression curve; this was shown to be due to beam-air

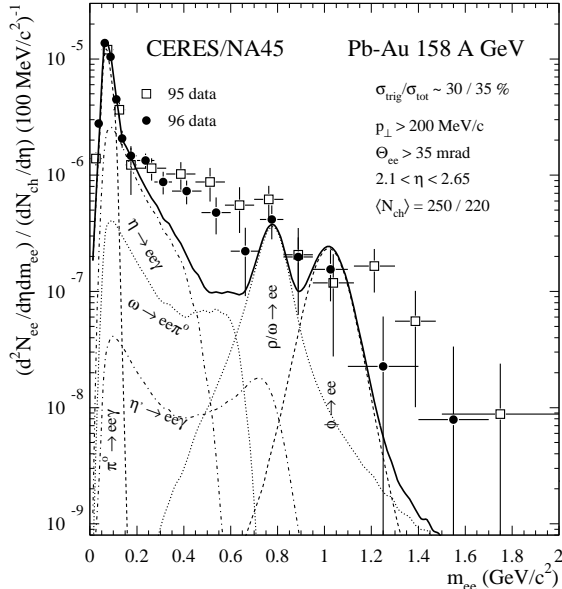


Figure 4. The dilepton spectrum in Pb-Au collisions at  $\sqrt{s} = 17$  GeV, compared to the expected yield (solid line) from known hadronic sources [ 23].

interactions and is no longer the case in the data collected in year 2000, when the target was placed in vacuum [ 22].

The dilepton mass spectrum in the region below the  $\rho$  peak was indeed found to differ considerably from the yield and form expected from known hadronic sources [ 23], indicating the presence of in-medium resonance modifications (Fig. 4). This ‘low mass dilepton enhancement’ is observed in S-U and Pb-Pb collisions, and for the latter at beam energies of 40 GeV as well as of 160 GeV. The broadening of transverse momentum spectra, expected as consequence of transverse flow, was observed in the predicted form of increasing broadening with hadron mass. If parametrized in terms of radial flow [ 24], the extracted flow velocity  $\beta_T$  appears to saturate with increasing collision energy (Fig. 5).

The transverse momentum spectra, moreover, also showed the azimuthal anisotropy predicted for non-central collisions. The behavior shown in Fig. 6 indicates at low collision energy a reduced emission in the transverse direction, where spectator nucleons are present; at high energy, there is enhanced production in the direction of the higher pressure gradient as determined by the anisotropic interaction volume [ 25].

The expected increase of source size in HBT correlation studies has not been observed; instead, one finds that, with increasing collision energy, the observed source radii are essentially determined by those of the involved nuclei [ 26]. Thus one finds  $R_{\text{side}} \simeq R_{\text{out}} \simeq 5 - 6$  fm for Au-Au/Pb-Pb collisions from AGS to SPS (and on to RHIC), as seen in Fig. 7. This is to be contrasted to predicted values for Pb-Pb collisions ranging from 14 fm for the SPS to 20 fm for RHIC, if freeze-out occurs when the mean free path of a hadron exceeds the system size [ 27]

$$R_f \simeq 0.7 \left( \frac{dN_h}{dy} \right)^{1/2}. \quad (2)$$

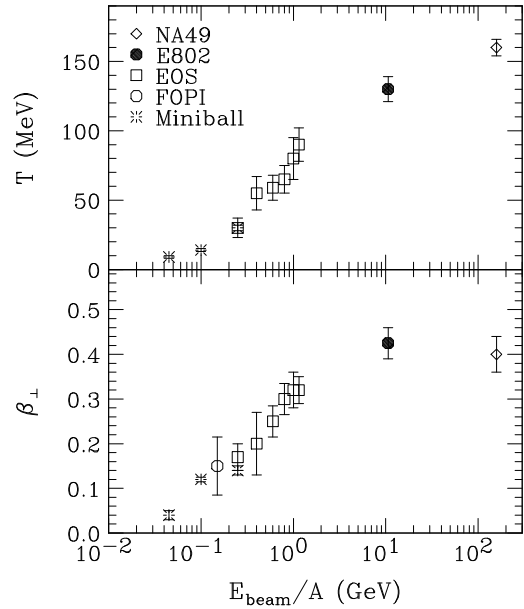


Figure 5. Hadronization temperature,  $T$ , and transverse flow measure,  $\beta_T$ , as function of the beam energy [ 24].

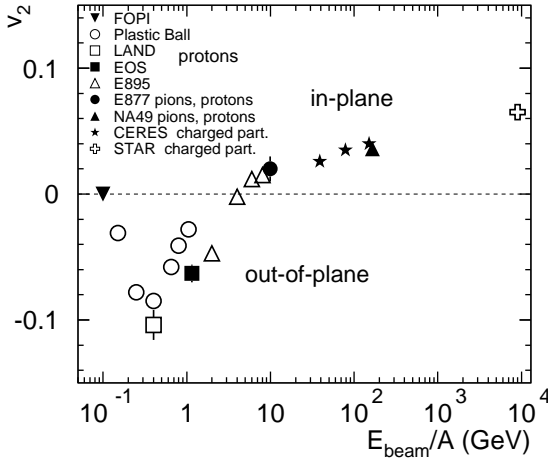


Figure 6. Elliptic flow measure,  $v_2$ , as function of the beam energy [ 25].

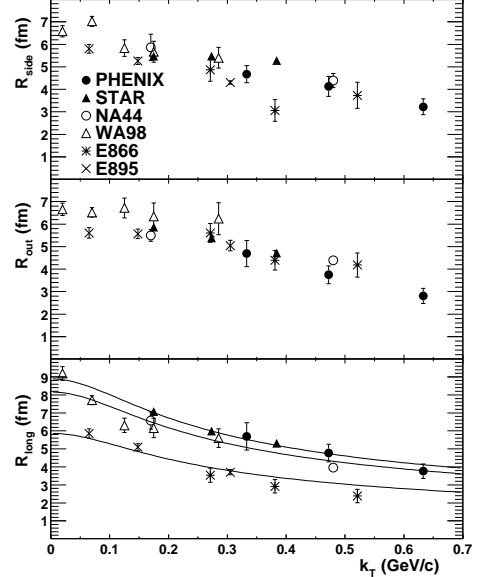


Figure 7. HBT radii at different collision energies [ 26].

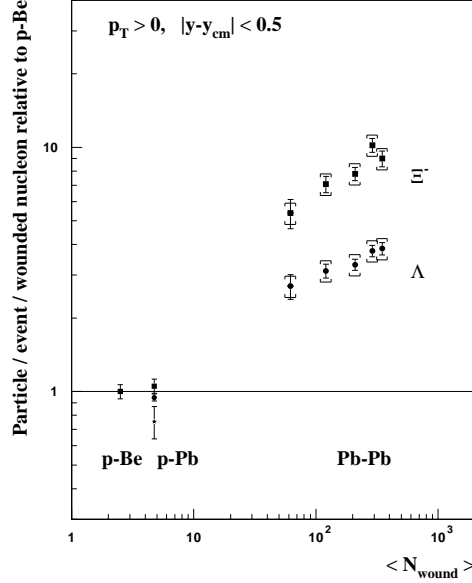
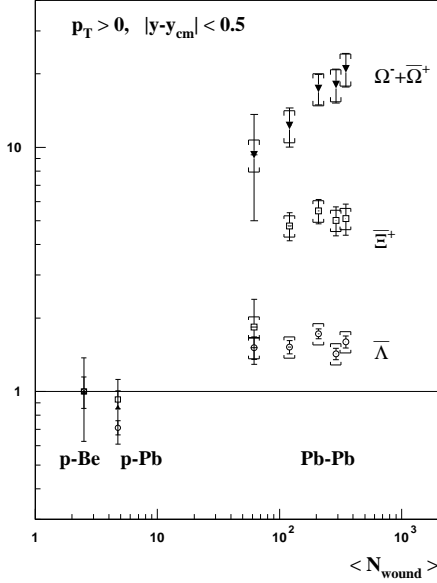


Figure 8. Strange hyperon production per participant nucleon, normalized to the ratio from p-Be, as function of the number of participant nucleons, as measured by NA57 [ 29].

For a freeze-out at the ideal pion gas energy density, one has  $R_f \sim (dN_h/dy)^{1/3}$ , which increases from 9 to 12 fm between SPS and RHIC energies. Another unexpected feature is that the outward and sideward radii,  $R_{\text{out}}$  and  $R_{\text{side}}$ , whose difference could provide information about the life-time of the emitting medium, appear to be approximately equal. The HBT source radii in nuclear collisions thus seem to be energy-independent and fixed by the initial nuclear size [ 28].

Hadron abundances showed the expected enhancement of strangeness production; in Fig. 8 we show the most striking example, where the production of strange baryons is



increased up to 10 times and more in comparison to  $pp$  rates [ 29]. In Fig. 9, it is seen that, quite generally, the Wroblewski measure for strangeness content is about a factor two higher in  $AA$  collisions than in elementary particle reactions. Of course, the role of the changing baryon density has to be kept in mind when comparing strangeness production in  $pp$  and  $AA$  collisions, or among  $AA$  collisions of different energies.

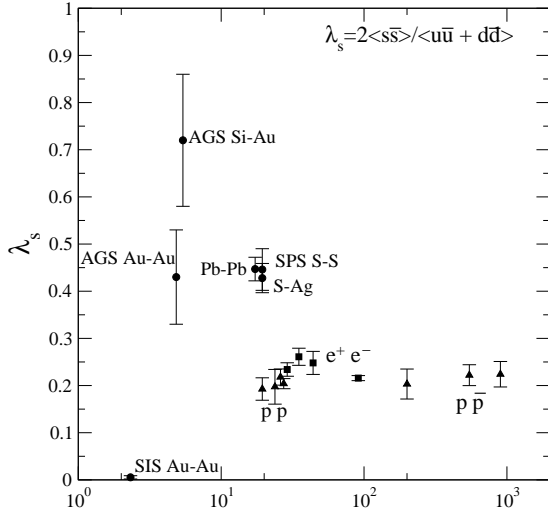


Figure 9. Wroblewski strangeness measure for different collision configurations [ 30].

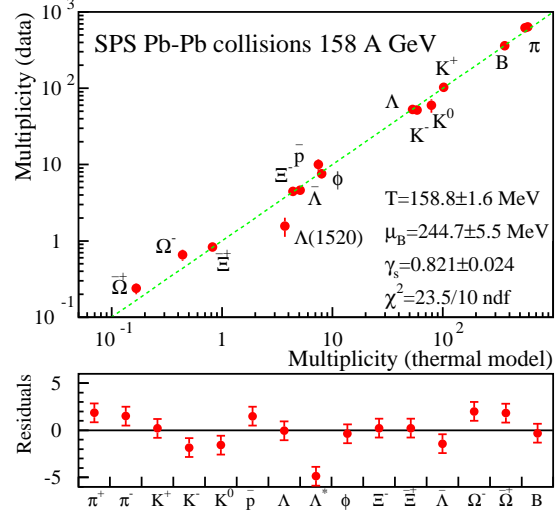


Figure 10. Thermal hadronization and species abundances, from Ref. [ 31].

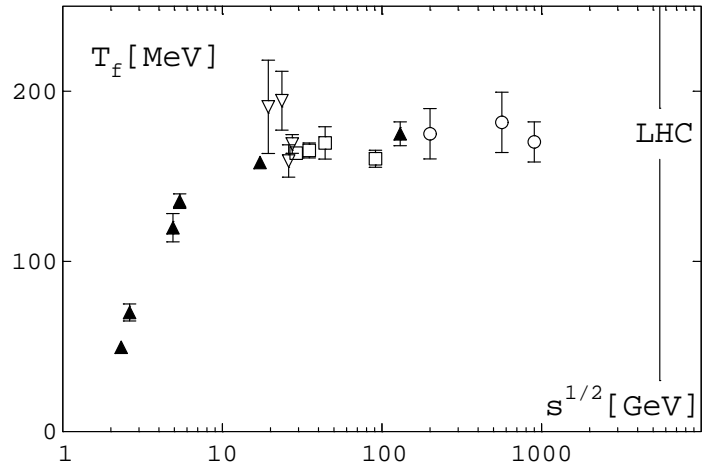


Figure 11. Hadronization temperature as function of c.m.s. energy, for  $e^+e^-$  (squares),  $pp$  (open triangles),  $p\bar{p}$  (circles) and  $AA$  collisions (filled triangles) [ 32].

Nevertheless, in all cases the abundance of the different hadron species is very well described by an ideal resonance gas. A fit to the latest NA49 data is shown in Fig. 10 [ 31]. The hadronization temperature increases with increasing collision energy and converges for all hadron production, from  $e^+e^-$  and  $pp/p\bar{p}$  to high energy  $AA$  collisions, to a stable value around 150–180 MeV; see Figs. 5 and 11. The associated baryo-chemical potential decreases when going from AGS to SPS and on to RHIC.

#### 4. Lessons

What can we learn from the results just listed? On the one hand, this is still a rather subjective issue, and so I proceed with due apologies to all those who feel that I have misunderstood what nature is trying to tell us. On the other hand, our theoretical understanding is presently at what might be a crucial point. It was and is generally thought that high energy nuclear collisions will produce a thermalized medium of deconfined quarks and gluons, so that we can test the predictions of finite temperature statistical QCD. In recent years, however, the role of the primary parton state has been emphasized in two independent but closely related approaches, color glass condensation [ 33, 34] and parton percolation [ 35, 36]. We are thus today confronted with the interesting question of knowing what part of the observable features of nuclear collisions are determined by the primary initial conditions, before any thermalization may take place.

Assuming thermal equilibration, with  $\tau_0 \simeq 1$  fm, the initial energy densities in central Pb-Pb collisions at the SPS are estimated to reach  $3$  GeV/fm $^3$  or more. What kind of medium can we have at this stage — could it be hadronic matter, a system of hadronic comovers of some kind? I believe that the answer is a clear NO. The average energy per hadron in these reactions is around  $0.5$  GeV, so that the mentioned energy density estimates would imply a hadron density of some  $6$  hadrons/fm $^3$ . The hadronic mean free path in such a medium,  $\lambda = 1/n_h \sigma_h$ , reaches something like  $\lambda \simeq 0.06$  fm, with a typical hadron-hadron interaction cross section of around  $30$  mb. The time needed by a hadron to react to a single collision is around  $1$  fm, and in that time it travels a distance  $\sim 1$  fm. In other words, the hadron undergoes almost twenty collisions in the time it needs to react to a single one. This rules out any medium consisting of independent hadrons [ 1, 37].

If the produced medium is not hadronic, does that mean that it is a quark-gluon plasma? The answer is not as easy as we once thought, so let us approach this problem slowly and carefully.

In a comparative study of the hadronization temperature  $T_H$  as function of the initial energy density for different production processes, from  $e^+e^-$  and  $pp/p\bar{p}$  reactions up to the heaviest  $AA$  collisions, we have to take into account the different values of the associated baryo-chemical potential. Since in all cases hadronization can be described in terms of an ideal resonance gas, we can extrapolate the baryon-rich low energy  $AA$  results at constant entropy to  $\mu_B = 0$ ; the resulting behavior is shown in Fig. 12 [ 38]. It is quite striking: above some threshold value  $\epsilon_c \simeq 1$  GeV/fm $^3$ , putting more energy into the system has no effect on the critical temperature  $T_H$  which determines the hadron abundances. In the end, Hagedorn was right [ 2]. This is like observing that water vapor always condenses to water at  $100^\circ\text{C}$ , whatever was the initial temperature of the vapor. While this shows that the water at the condensation point gives no information about the earlier vapor temperatures, it also indicates that the condensation process exhibits critical behavior. In the same way, a constant  $T_H$  for hadronic matter of arbitrarily high energy densities appears to signal critical behavior [ 4]. With this in mind, we now look once more at the experimental numbers. The saturation temperature is  $150$ – $180$  MeV, and is reached for  $\epsilon \simeq 1$  GeV/fm $^3$ ; both values are in excellent agreement with the mentioned results from lattice QCD studies [ 5]. For very small or vanishing baryon density, experiment and theory thus fully agree on the boundary of hadron physics.

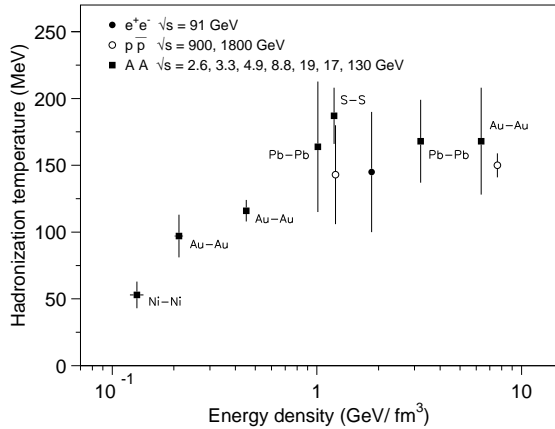


Figure 12. Hadronization temperature vs. the initial energy density, from Ref. [ 38].

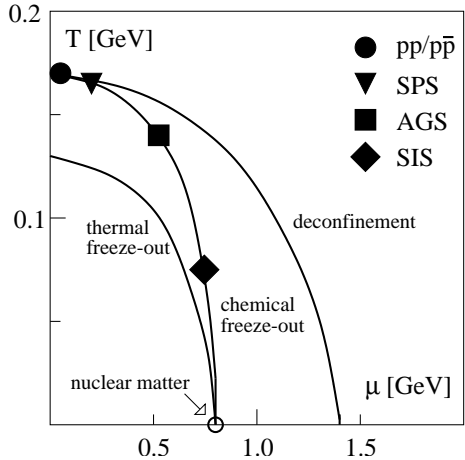


Figure 13. Deconfinement, chemical and thermal freeze-out vs.  $T$  and  $\mu$  [ 41, 42].

Extending the resonance gas analysis of species abundances to finite baryon density, one obtains the ‘chemical’ freeze-out curve [ 39, 40] in the  $T - \mu_B$  plane; it is illustrated schematically in Fig. 13. Also included in this figure are the thermal freeze-out curve (obtained from a flow analysis of transverse momentum spectra) and the expected deconfinement transition curve [ 41]. Some first and quite promising attempts of lattice gauge theory to study deconfinement at non-zero baryo-chemical potential,  $\mu_B$ , agree with the deconfinement curve for  $\mu_B \leq 0.8$  GeV [ 43, 44]. It is clear that the deconfinement curve must lie above the freeze-out curve at large  $\mu_B$ : the interactions in cold dense nuclear matter are dominated by baryon repulsion and hence cannot be described in terms of an ideal resonance gas. At  $T=0$ , freeze-out occurs at normal nuclear matter density, where baryon repulsion and attractive (pion exchange) interactions just balance each other. Neutron stars are examples of confined states of higher baryon densities.

Since Figs. 11, 12 and 13 include both data from elementary particle and from nuclear collisions, statistical hadron abundances alone are not sufficient to indicate the presence of a large-scale system. Therefore, it is necessary to check if  $AA$  collisions produce large thermal systems or just the sum of the smaller ones. The answer to that question is obtained through the study of strangeness production. In elementary particle collisions, there is an overall suppression of strange particle production compared to the predictions of the grand canonical form of an ideal resonance gas. This can be interpreted as the consequence of local strangeness conservation: if only one  $s\bar{s}$  pair is formed in the gas, the corresponding Boltzmann factor should be  $\exp\{-2m_s/T\}$ , instead of the grand canonical form  $\exp\{-m_s/T\}$ . If nuclear collisions lead to a connected large-scale system, strangeness conservation can occur between the products from different nuclei, leading to the grand canonical Boltzmann factor. As a consequence, we expect for the Wroblewski measure in elementary particle collisions

$$\lambda_s \equiv \frac{2 \langle s\bar{s} \rangle}{\langle u\bar{u} \rangle + \langle d\bar{d} \rangle} \simeq \exp\{-2m_s/T\} \simeq 0.2, \quad (3)$$

while central high energy  $AA$  collisions should approach

$$\lambda_s \simeq \exp\{-m_s/T\} \simeq 0.4. \quad (4)$$

Keeping in mind that the different baryon densities also lead to modifications, we see in

Fig. 9 that Eqs. (3) and (4) are in fact quite well satisfied. We thus conclude that nuclear collisions indeed produce large-scale connected systems.

The observed behavior of the hadronic transverse momentum spectra is also often taken as indication for collective behavior of the produced medium. In particular, azimuthal asymmetries seem to indicate that global effects influence the spatial hadron emission: in non-central collisions, there is more (elliptic) flow in the direction of the greater pressure gradient. For the time being, however, it is not so easy to reconcile a constant radial flow velocity at high energy (Fig. 5) and energy-independent HBT radii of nuclear size (Fig. 7) with an initial state of partonic matter at higher and higher energy densities. Apparently a change of conditions in the pre-hadronic phase, whatever its nature, is not reflected in radial flow or source size.

We conclude that there seems to be a universal limit to the hadronization regime in high energy nuclear collisions; the abundances of the produced hadron species, including the strange ones, are determined by values of temperature and energy density in good agreement with what is known about the confined region of the QCD phase diagram. As function of the incident energy, the hadronization temperature  $T_H$ , the strangeness content  $\lambda_s$  and the transverse momentum broadening (radial flow velocity  $\beta_T$ ) all seem to converge to constant values. The value of the temperature  $T_H \simeq 150 - 180$  MeV and of the corresponding energy densities agree with the confinement/deconfinement transition values obtained in lattice QCD. The strangeness content agrees with what is expected from the value of the Boltzmann factor  $\exp\{-m_s/T\}$  at  $T = T_H$ . In fact, even the low mass dilepton enhancement appears to remain essentially invariant under changes of nuclear size and of collision energy (in the SPS range). The origin of the effect is not yet really clear (see, however, [ 45]), but low mass dilepton production does seem to behave in the same way as the mentioned hadronic observables. Since it may be the most sensitive to changes in the initial baryon density [ 46], this observation could be a reflection of the weak  $\mu$ -dependence of the confinement limit in the small  $\mu$  region.

Before analyzing the earlier stages of the nuclear collisions, we briefly mention attempts to include charmonium production in a statistical hadronization scheme, either by assuming thermal formation at the freeze-out point  $T = T_H$  of the resonance gas [ 47], or by assuming a thermal distribution of the produced  $c\bar{c}$  pairs among the different possible open and hidden charm channels [ 48]. To evaluate the viability of these approaches, we recall that  $J/\psi$  production from  $pp$  to central S-U and peripheral Pb-Pb collisions is seen to be in accord with the normal nuclear suppression determined in p-A interactions. In contrast, more central Pb-Pb collisions show a well-defined onset of anomalous suppression in a narrow centrality range, seen both in the ratio of  $J/\psi$  to Drell-Yan production and in the overall  $J/\psi$  yield (see Fig. 3). Such an onset cannot be obtained in any thermal production model, nor can the centrality-dependent  $\psi'/\psi$  ratio found in S-U collisions [ 49]. Hence, the present data indicate that the production and subsequent fate of charmonium states in nuclear collisions differ significantly from that of light hadrons. We shall return shortly to the interpretation of the observed charmonium patterns.

The study of the behavior of (light quark) hadrons has thus provided us with clear indications determining where the hadronic regime ends. It does not tell us, however, where the QGP begins. High energy elementary particle collisions lead to initial energy density estimates higher than those of Pb-Pb collisions at SPS or RHIC energies (see

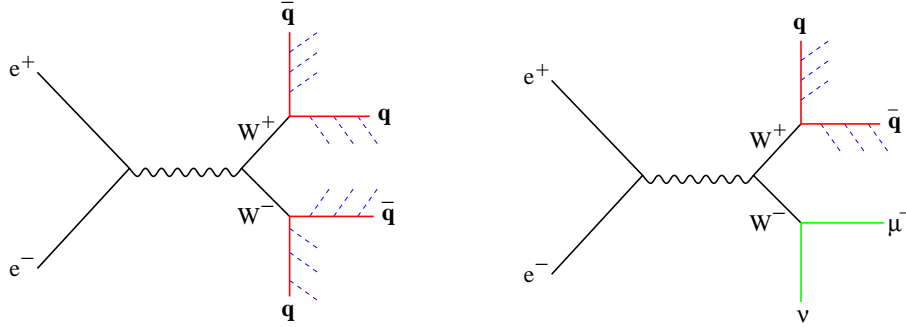


Figure 14. Four-jet and two-jet decays of  $W^+W^-$  pairs in  $e^+e^-$  annihilation at LEP.

Fig. 12); for the resulting hadronization temperatures we always get the universal  $T_H$ . Therefore, one has tried to find evidence for pre-hadronic interactions, between partons from different sources. In  $e^+e^-$  interactions at LEP energies ( $\sqrt{s} \simeq 200$  GeV), this can be done by comparing hadron multiplicities in two-jet and four-jet decays of  $W^+W^-$  pairs produced essentially at rest (see Fig. 14). ‘Cross talk’ between jets from different  $W$ ’s should be reflected in hadron multiplicities, with the prediction [ 50] that  $N_h(4jet) < 2N_h(2jet)$ . The data do not show any evidence for such ‘color interconnection’ [ 51], even though the energy density calculated according to the Bjorken estimate (1) reaches values around  $2$  GeV/fm $^3$ . The partons from different sources simply don’t seem to know of each other. Color interconnection is clearly a prerequisite for thermalization on a partonic level; hence  $\epsilon \geq 1$  GeV/fm $^3$  is a necessary, but not a sufficient condition for QGP formation. We must somehow assure that the partons in the early stages of the collision reach a density so high that they interact and allow color interconnection to set in. In other words, the pertinent question is: when do the individual partons from the different nucleons of the colliding nuclei condense to form a large connected cluster?

From percolation theory [ 52], it is known that the formation of large-scale clusters is a critical phenomenon; it does not occur gradually as function of parton density. In the ‘thermodynamic’ limit of large nuclei, the cluster size diverges at a specific critical parton density, and even for finite systems it suddenly increases in a very narrow band of density. Thus there exists a statistical approach to critical behavior which does not pre-suppose thermalization and which can be applied to the pre-equilibrium stage of the nuclear collision evolution [ 35, 36].

In a central high energy nucleus-nucleus collision, the partons in the two nuclei lead in the transverse plane to an initial condition schematically illustrated in Fig. 15. The trans-

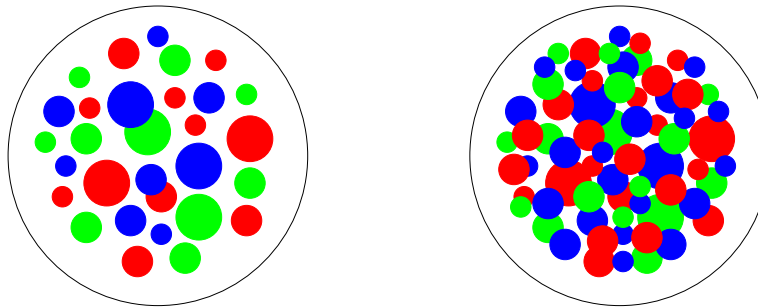


Figure 15. Parton distribution in the transverse plane of a nucleus-nucleus collision, for small (left) and large (right) nuclei.

verse size of the partons is essentially determined by the intrinsic transverse momentum,  $\sigma_q \sim \pi/k_T^2$ . The number of partons contained in a nucleon is known from deep inelastic scattering experiments. It is parametrized by a parton distribution function depending on the fraction  $x = k/p$  (denoting parton and nucleon momenta by  $k$  and  $p$ , respectively) and on the scale  $Q$  used to resolve the nucleonic parton structure. While in lepton-hadron scattering the scale is set by the virtual photon, in minimum bias nucleon-nucleon or  $AA$  collisions it is determined by the transverse momentum of the partons themselves.

We denote the nuclear radius in Fig. 15 by  $R$ , the average parton radius by  $r$ , and then study the variation of the average cluster size as function of the parton density  $n = N_{\text{parton}}/\pi R^2$ . In the limit  $R \rightarrow \infty$ , the cluster size diverges at the percolation threshold  $n_p \simeq 1.13/\pi r^2$ :

$$S_{\text{cl}} \sim (n_p - n)^{-\gamma}, \quad (5)$$

with the critical exponent  $\gamma = 43/18$  [53]. Percolation thus specifies the onset of connection as a critical phenomenon. For finite  $R$ , there is a pronounced but finite peak at a slightly shifted density, as shown in Fig. 16.

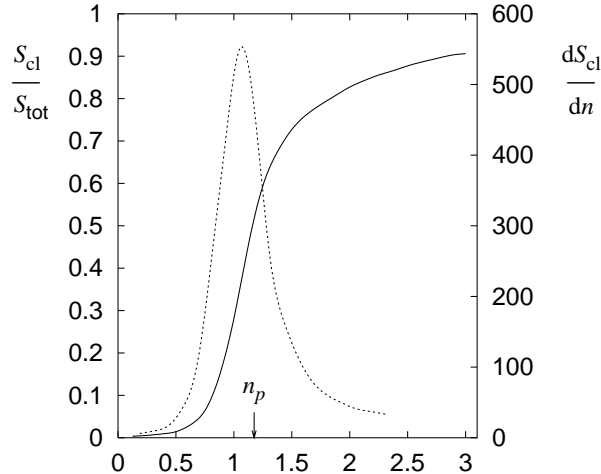


Figure 16. Average cluster size  $S_{\text{cl}}$  as function of parton density  $n$ ;  $n_p$  denotes the percolation point in the limit  $R \rightarrow \infty$ .

To apply this formalism to nuclear collisions [36], we need the transverse parton size and the effective number of partons for a given collision configuration. The distribution of partons in a nucleon is determined in the analysis of deep inelastic scattering data; per nucleon in a nucleon-nucleon collision, at mid-rapidity and for c.m.s. energy  $\sqrt{s}$ , one has

$$N_{\text{parton}}(x, Q^2) = \left( \frac{dN_q}{dy} \right)_{y=0} = xg(x, Q^2) + \sum [xq(x, Q^2) + x\bar{q}(x, Q^2)], \quad (6)$$

where  $g, q, \bar{q}$  label the gluon, quark and antiquark distributions, respectively, and the sum runs over the quark species. At  $y = 0$ , the fractional parton momentum  $x = k/p$  becomes  $x = Q/\sqrt{s}$ . As shown in Fig. 15, there is a distribution of partons of different transverse sizes up to the resolution scale  $Q^2$ ; we approximate this by the average value  $\pi \langle r^2 \rangle \simeq \pi/Q^2$ .

In nucleus-nucleus collisions at SPS energies, it is a good approximation to consider that the activated partons originate from wounded or participant nucleons. At higher energies, there will also exist collision-dependent contributions [ 54].

We thus obtain for central  $AA$  collisions the percolation condition

$$\frac{2A}{\pi R_A^2} N_{\text{parton}}(x, Q^2) = \frac{1.13}{\pi Q^{-2}}; \quad (7)$$

it determines the onset of color connection as function of  $A$  and of the c.m. collision energy  $\sqrt{s}$ . At  $\sqrt{s} = 20$  GeV, we obtain [ 36]:

$$\begin{aligned} \text{for } A \lesssim 60, & \text{ no color connection,} \\ \text{for } A \gtrsim 60, & \text{ a connected parton condensate.} \end{aligned}$$

The parton condensate formed beyond the percolation point consists of overlapping and hence interacting partons from all involved nucleons. It thus constitutes a deconfined pre-thermal medium, which is a necessary precursor for QGP formation, since color connection is a prerequisite for thermalization. The parton condensate is characterized by a scale  $Q = Q_s$ , where  $Q_s(A, \sqrt{s})$  specifies the onset of percolation for central collisions at a given  $A$  and  $\sqrt{s}$ . The average transverse momentum of partons in the condensate is determined by this scale, so that  $Q_s$  is in a sense a precursor of temperature. Increasing  $A$  or  $\sqrt{s}$  leads to higher  $Q_s$ , indicating something like a “hotter” medium.

We have here concentrated on the onset of parton condensation as a critical phenomenon determined by percolation of quarks and gluons as geometric entities in the transverse plane. The behavior of the dense parton condensate in the limit of large  $A$  and  $\sqrt{s}$ , the color glass condensate, has been studied intensively over the past years in terms of classical color fields. It is becoming increasingly clear from these studies that the pre-equilibrium stage plays a much more decisive role in nuclear collisions than previously envisioned. In the last part of this section, we consider one interesting experimental consequence of the onset of parton condensation.

To study this onset as function of centrality in a given  $A - A$  collision, we have to replace  $2A/\pi R_A^2$  in Eq. (7) by the density of wounded nucleons  $n_w(b)$  calculated for a given impact parameter  $b$ , using the actual nuclear profile (Woods-Saxon). For Pb-Pb collisions at  $\sqrt{s} = 17$  GeV, this leads to

$$\begin{aligned} \text{for } N_w \lesssim 150, & \text{ no color connection,} \\ \text{for } N_w \gtrsim 150, & \text{ a connected parton condensate.} \end{aligned}$$

Instead of the impact parameter, we have here used the number of wounded nucleons to specify the collision centrality, with  $N_w \simeq 390$  for  $b = 0$ . Note that at this threshold point, the Bjorken estimate for the energy density gives  $\sim 2.5$  GeV/fm $^3$ . This clearly shows that the onset of color connection only occurs at a much higher energy density than the value given by finite temperature lattice QCD for a thermalized medium.

As mentioned above, charmonium suppression in nuclear collisions was one of the proposed signatures for quark-gluon plasma formation. In the light of present thinking, we have to consider the fate of the charmonium states already in the parton condensate phase. This can be addressed in different ways, invoking generalized color screening [ 55], dipole break-up in a random color field [ 56], etc. We shall here simply consider the intrinsic scale  $Q_i$  of a given charmonium state  $i$  ( $J/\psi$ ,  $\chi_c$ ,  $\psi'$ ) and assume that when it is

exceeded by the condensate scale,

$$Q_s > Q_i, \quad (8)$$

the charmonium state is dissolved. We are thus assuming that  $Q_s$  plays in the pre-equilibrium state the role of the critical temperature or of the screening mass in a thermal medium.

To show the consequences of this assumption, we must first recall that  $J/\psi$  production in hadronic collisions occurs in part through feed-down from higher excited states: about 60% of the observed  $J/\psi$  in proton-proton collisions are directly produced ( $1S$ ) states, the remaining 40% coming from  $\chi_c$  ( $\sim 30\%$ ) and  $\psi'$  ( $\sim 10\%$ ) decays. The intrinsic scales of these states are given by their radii,

$$r_{J/\psi} \simeq (0.9 \text{ GeV})^{-1}, \quad r_{\chi} \simeq (0.6 \text{ GeV})^{-1}, \quad r_{\psi'} \simeq (0.6 \text{ GeV})^{-1}. \quad (9)$$

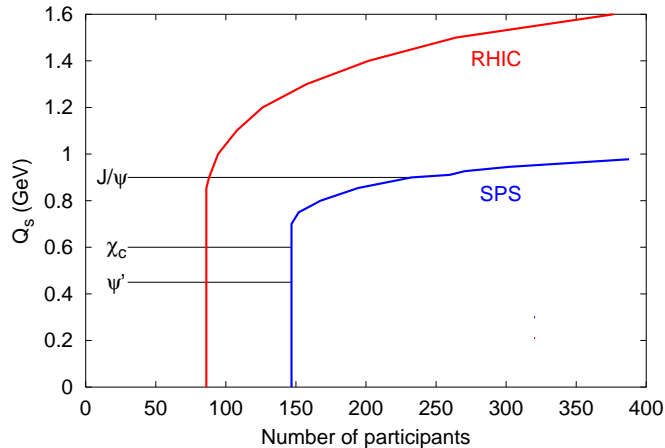


Figure 17. Centrality dependence of the percolation scale,  $Q_s$ , in Pb-Pb collisions, at SPS and RHIC energies [ 36].

From the centrality dependence of  $Q_s$  shown in Fig. 17, we find that, at SPS energies, charmonia suppression sets in at

$$\begin{aligned} N_w &\gtrsim 150 \text{ for the } \chi_c \text{ and } \psi' \text{ contributions,} \\ N_w &\gtrsim 250 \text{ for direct } J/\psi \text{ production,} \end{aligned}$$

to be compared with the observed pattern shown in Fig. 18. Obviously these results must be studied in more detail, but it appears quite likely that the onset of  $J/\psi$  suppression indeed indicates an onset of deconfinement, while not implying any thermalization.

## 5. Summary

So let us summarize what we have learned in the first fifteen years of ultra-relativistic heavy ion collisions.

We know that there is an intrinsic limit to hadronic matter, in accord with the phase diagram determined in statistical QCD. The confinement boundary is established by the SPS/AGS program and agrees, both qualitatively and quantitatively, with the predictions of lattice QCD. I believe that the RHIC and LHC experiments can only reconfirm this. For

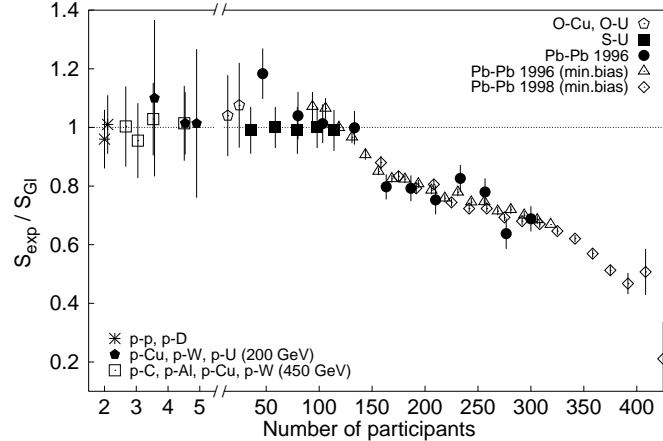


Figure 18.  $J/\psi$  production in  $pp$ ,  $p$ - $A$  and  $AB$  collisions, as function of the number of wounded nucleons [ 16].

small  $\mu_B$ , we know the onset of hadronization, and we know that strangeness enhancement, transverse momentum broadening and HBT radii saturate at this onset.

The early stage of the medium produced in nuclear collisions at the SPS is partonic. With increasing  $A$ , the partons begin to form connected clusters, and at a certain critical density, they form a color condensate consisting of interacting partons from many different nucleons. Hence, at this point, color deconfinement begins: partons no longer have a clear origin or exist in well-defined numbers. The parton condensate is a necessary precursor of the QGP: it provides the interacting deconfined partons which, if given enough time for equilibration, can make a QGP.

Charmonium states of different binding energies and spatial sizes probe different parton scales of the produced initial state. The observed step-wise form of anomalous  $J/\psi$  suppression appears to provide the first signal for color deconfinement through parton condensation; this does not require any thermalization. The forthcoming  $J/\psi$  production measurements at full SPS energy but with lower  $A$ , to be performed by NA60, should further clarify this point. In particular, the comparison between Pb-Pb and In-In  $J/\psi$  suppression patterns should determine the critical densities and scales.

Pioneering results in physics always need to be reconfirmed. But if these limits of confinement survive the test of time, we will remember that they were first found in SPS/AGS experiments.

So, at the beginning of the collision evolution at the SPS, there appears to be color deconfinement; at the end, thermalization and collective behavior. To produce a quark-gluon plasma medium, we need to have both at the early stage. Let us see if the future data from experiments at the much higher RHIC and LHC energies can achieve this. But no matter how well-defined the road for further exploration may seem to be, I am sure that the forthcoming studies will rediscover the one feature which has made this field so challenging and exciting. It is perhaps best summarized by the Spanish poet Antonio Machado [ 57]:

*Caminante, son tus huellas el camino, y nada más;  
caminante, no hay camino, se hace camino al andar.*

*Traveller, the road is nothing more than your footprints;  
traveller, there is no road, you make it as you go.*

## Acknowledgements

It is a pleasure to acknowledge the help of many colleagues in the preparation of this survey; special thanks go to P. Braun-Munzinger, S. Digal, S. Fortunato, F. Karsch, D. Kharzeev, M. Nardi, P. Petreczky, K. Redlich, H. Specht, U. Wiedemann and, in particular, to C. Lourenço. I am grateful to L. Vázquez for literary support.

## REFERENCES

1. I.Ya. Pomeranchuk, *Dokl. Akad. Nauk SSSR* 78 (1951) 889.
2. R. Hagedorn, *Nuovo Cim. Suppl.* 3 (1965) 147.
3. S. Fubini and G. Veneziano, *Nuovo Cim.* 64 A (1969) 811;  
K. Bardakçi and S. Mandelstam, *Phys. Rev.* 184 (1969) 1640.
4. N. Cabibbo and G. Parisi, *Phys. Lett.* 59 B (1975) 67.
5. For a recent survey, see F. Karsch, *Nucl. Phys.* A698 (2002) 199c.
6. J.D. Bjorken, *Phys. Rev.* D27 (1983) 140.
7. E.V. Shuryak, *Phys. Rep.* 61 (1980) 71.
8. K. Kajantie and H.I. Miettinen, *Z. Phys. C* 9 (1981) 341;  
K. Kajantie et al., *Phys. Rev.* D34 (1986) 2746.
9. T. Matsui and H. Satz, *Phys. Lett.* B178 (1986) 416.
10. J.D. Bjorken, Fermilab-Pub-82/59-THY (1982) and Erratum;  
M. Gyulassy and X.-N. Wang, *Nucl. Phys.* B420 (1994) 583.
11. R. Pisarski, *Phys. Lett.* B110 (1982) 155;  
V. Bernard et al., *Phys. Lett.* B227 (1989) 465;  
G.E. Brown et al., *Phys. Rev.* C43 (1991) 1881.
12. L. Van Hove, *Phys. Lett.* B118 (1982) 138;  
M. Kataja et al., *Phys. Rev.* D34 (1986) 2755.
13. M. Gyulassy et al., *Phys. Rev.* C20 (1979) 2267.
14. E. Beth and G.E. Uhlenbeck, *Physica* 4 (1937) 915.
15. B. Müller and J. Rafelski, *Phys. Rev. Lett.* 48 (1982) 1066;  
J. Rafelski, *Phys. Rep.* 88 (1982) 331;  
P. Koch, B. Müller and J. Rafelski, *Phys. Rep.* 142 (1986) 168.
16. M.C. Abreu et al. (NA50), *Phys. Lett.* B410 (1997) 337;  
M.C. Abreu et al. (NA50), *Phys. Lett.* B450 (1999) 456;  
M.C. Abreu et al. (NA50), *Phys. Lett.* B477 (2000) 28.
17. M. Nardi, private communication.
18. M.M. Aggarwal et al. (WA98), *Phys. Rev. Lett.* 85 (2000) 3595.
19. E. Scomparin et al. (NA50), *Nucl. Phys.* A610 (1996) 331c;  
N. Masera et al. (HELIOS-3), *Nucl. Phys.* A590 (1995) 93c.
20. R. Rapp and E. Shuryak, *Phys. Lett.* B473 (2000) 13.
21. C. Baglin et al. (NA38), *Phys. Lett.* B220 (1989) 471;  
M.C. Abreu et al., *Phys. Lett.* B410 (1997) 337.
22. L. Ramello, in these (QM2002) proceedings.
23. G. Agakichiev et al. (CERES), *Phys. Rev. Lett.* 75 (1995) 1272;  
G. Agakichiev et al. (CERES), *Phys. Lett.* B422 (1998) 405;  
B. Lenkeit et al. (CERES), *Nucl. Phys.* A661 (1999) 23c.

24. Compilation by P. Danielewicz, Nucl. Phys. A685 (2001) 368.
25. Compilation by H. Appelshäuser, Nucl. Phys. A698 (2002) 253.
26. Compiled in K. Adcox et al. (PHENIX), Phys. Rev. Lett. 88 (2002) 192302.
27. A.Z. Mekjian, Phys. Rev. C17 (1978) 1051;  
see also H. Satz, in CERN 90-10 (Proc. of the LHC Workshop, Aachen 1990).
28. For a recent account of the observed behavior, see  
D. Adamová et al. (CERES), nucl-ex/0207008.
29. K. Fanebust et al. (NA57), J. Phys. G 28 (2002) 1607;  
F. Antinori and V. Manzari, private communication.
30. F. Becattini et al., Phys. Rev. C64 (2001) 024901.
31. Analysis by F. Becattini, data from M. van Leeuwen et al. (NA49), nucl-ex/0208014.
32. H. Satz, Rep. Prog. Phys. 63 (2000) 1511.
33. L. McLerran and R. Venugopalan, Phys. Rev. D49 (1994) 2233;  
L. McLerran and R. Venugopalan, Phys. Rev. D49 (1994) 3352.
34. L. McLerran, hep-ph/0202025;  
E. Iancu et al., hep-ph/0202270.
35. H. Satz, Nucl. Phys. A661 (1999) 104c.
36. S. Digal et al., hep-ph/0207264.
37. See e.g., E.L. Feinberg and I.Ya. Pomeranchuk, Nuovo Cim. Suppl. 3 (1956) 652.
38. S. Kabana, hep-ph/0111394.
39. P. Braun-Munzinger and J. Stachel, Nucl. Phys. A606 (1996) 320;  
P. Braun-Munzinger and J. Stachel, Nucl. Phys. A638 (1998) 3.
40. J. Cleymans and K. Redlich, Phys. Rev. C60 (1999) 054908.
41. P. Braun-Munzinger and J. Stachel, nucl-th/0112051.
42. K. Redlich, private communication.
43. Z. Fodor and S.D. Katz, hep-lat/0104001; hep-lat/0106002.
44. C.R. Allton et al., hep-lat/0204010.
45. M. Urban et al., Nucl. Phys. A673 (2000) 357;  
G. E. Brown and M. Rho, nucl-th/0206021.
46. See e.g., J. Wambach, Nucl. Phys. A699 (2002) 10.
47. M. Gazdzicki and M. Gorenstein, Phys. Rev. Lett. 83 (1999) 4009.
48. P. Braun-Munzinger and J. Stachel, Phys. Lett. B490 (2000) 196.
49. M.C. Abreu et al. (NA38), Phys. Lett. B466 (1999) 408.
50. J.R. Ellis and K. Geiger, Phys. Lett. B404 (1997) 230.
51. For a recent survey, see P. Abreu, hep-ph/0111395.
52. See e.g., D. Stauffer and A. Aharony, *Introduction to Percolation Theory*, Taylor and Francis, London 1994.
53. M.B. Isichenko, Rev. Mod. Phys. 64 (1992) 961.
54. D. Kharzeev and M. Nardi, Phys. Lett. B507 (2001) 121.
55. V.P. Gonçalves, Phys. Lett. B518 (2001) 79.
56. H. Fuji and T. Matsui, nucl-th/0204065;  
H. Fuji, nucl-th/0205066.
57. Antonio Machado (1875 - 1939), *Poesías Completas: Proverbios y Cantares XXIX*.